Interactions of Small Nuclear RNA's with Precursor Messenger RNA During in Vitro Splicing

David A. Wassarman and Joan A. Steitz

Precursor messenger RNA splicing requires multiple factors including U1, U2, U4, U5, and U6 small nuclear RNA's. The crosslinking reagent psoralen was used to analyze the interactions of these RNA's with an adenovirus precursor messenger RNA in HeLa nuclear extract. An endogenous U2-U4-U6 crosslinkable complex dissociated upon incubation with precursor messenger RNA. During splicing, U1, U2, U5, and U6 became crosslinked to precursor messenger RNA and U2, U5, and U6 became crosslinked to excised lariat intron. U2 also formed a doubly crosslinked complex with U6 and precursor messenger RNA. The U1, U5, and U6 crosslinks to the precursor messenger RNA mapped to intron sequences near the 5′ splice site, whereas the U2 crosslink mapped to the branch site. The kinetics of crosslink formation and disappearance delineates a temporal pathway for the action of small RNA's in the spliceosome. Potential base pairing interactions between conserved sequences in the small nuclear RNA's and precursor messenger RNA at the sites of crosslinking suggest that the 5′ splice site is defined in several steps prior to the first cleavage event.

Precursor messenger RNA (pre-mRNA) splicing is the process by which introns are removed and exons joined to form mature mRNA (*1*). Splicing occurs by a two-step transesterification mechanism: in the first step, the 5′ splice site is cleaved to generate a 5′ exon and a lariat intermediate, and in the second, the 3′ splice site is cleaved to generate ligated exons (spliced product) and an excised lariat intron. This process is carried out in a dynamic complex called the spliceosome, composed of U1, U2, U4-U6, and U5 small nuclear ribonucleoproteins (snRNP's) and numerous non-snRNP protein factors. Assembly of these trans-acting factors into a spliceosome is directed in part by highly conserved pre-mRNA sequences at the 5′ and 3′ splice sites and the branch site.

Spliceosome assembly in vitro involves sequential binding of the U1 snRNP, the U2 snRNP and, finally, U4-U6 and U5 as a preformed U4-U5-U6 tri-snRNP (*1*). The U4 and U6 snRNP's associate via two extensive intermolecular RNA helices termed stems I and II. Prior to 5′ splice site cleavage, base-pairing between the U4 and U6 small nuclear RNA's (snRNA's) is unwound, which reduces the affinity of U4 for the spliceosome. Similarly, the affinity of U1 for the pre-mRNA is weakened prior to 5′ splice site cleavage. After the nucleolytic steps and exon ligation, the splice RNA is released and U2, U4, U5, and U6 remain associated with the excised lariat intron. Sequential RNA base pairing interactions in the spliceosome may be driven by ATP (adenosine triphosphate) hydrolysis, as a number of yeast splicing factors exhibit sequence similarities to ATP-dependent RNA helicases.

Base pairing between conserved snRNA and pre-mRNA sequences is required for spliceosome assembly and accurate, efficient splicing (*1*). Studies with mammalian and yeast systems have indicated that the 5′ end of U1 base pairs with the 5′ splice site, that a region near the 5′ end of U2 base pairs with the branch site, and that a snRNP, most likely U5, binds to the 3′ splice site. Genetic experiments with the yeast *Schizosaccharomyces pombe* suggest that additional base pairing occurs between the 5′ end of U1 and the 3′ splice site prior to the first step of splicing (*2*). Other analyses with a mutant splicing substrate of the yeast *Saccharomyces cerevisiae* (containing a G to A transition at invariant position 1 of the intron) indicate that base pairing between an invariant loop of U5 and less well conserved exon sequences at 5′ and 3′ splice sites may also occur (*3*, *4*). In mammalian systems, base pairing between the 3′ end of U6 and the 5′ end of U2 is required during splicing (*5*). Ultraviolet (UV) crosslinking studies have shown that a central region of U6 interacts with the 5′ splice site in the pre-mRNA and with sequences near the branch point adenosine in the excised lariat intron (*6*).

Previous studies with the crosslinking reagent psoralen have detected U1/heterogeneous nuclear RNA (hnRNA) and U2/hnRNA contacts in vivo (*7*), and U4/U6 (*8*) and U2/U6 (*9*) contacts in vitro [throughout this article crosslinks are denoted by a slash (/) and noncovalent interactions by a hyphen (-)]. However, these interactions have not been identified in active spliceosomes. We now document the appearance and disappearance of snRNA crosslinks during in vitro splicing, some of which reflect novel interactions of these RNA's with the pre-mRNA substrate. Our results suggest a defined pathway of intermolecular base pairing interactions required for catalysis, analogous to those in group II self-splicing RNA's.

A U2-U4-U6 complex in HeLa nuclear extracts. The psoralen derivative AMT (4′-aminomethyl-4,5′,8-trimethylpsoralen) is a useful probe for nucleic acid structure and function (*10*). Psoralen intercalates into DNA and RNA helices and upon irradiation with UV (365 nm) light forms a covalent link between pyrimidine (usually uridine) residues juxtaposed on opposite strands in a particular helical geometry. It can also crosslink non–base paired but closely associated RNA sequences in complex macromolecular assemblies (*11*). A valuable property of psoralen is that crosslinks can be photoreversed by irradiation with 254-nm light (*10*).

To identify endogenous snRNA-snRNA interactions in HeLa nuclear extracts, we performed psoralen crosslinking and subjected the reaction mixture to immunoprecipitation with antibodies to m_3G. These antibodies are directed against the 2,2,7-trimethylguanosine (m_3G) cap structure found on the U1, U2, U4, and U5 snRNA's, and therefore allow enrichment of these RNA's over more abundant species. The immunoprecipitated RNA's were 3′ end-labeled with [^{32}P]Cp (*12*) and fractionated on a two-dimensional gel system, in which the crosslinks were photoreversed with 254 nm light after the first dimension (Fig. 1). Uncrosslinked RNA's exhibit the same mobility in both dimensions and form a diagonal. Crosslinked RNA's migrate slower than RNA's of equivalent combined length in the first dimension and after photoreversal run off the diagonal, vertically to one another, in the second dimension.

In addition to previously identified U4/U6 and U2/U6 crosslinked complexes, a U2/U4/U6 complex was detected at a much lower level (Fig. 1). Quantitation of these three crosslinked species revealed that the abundance of the U2/U4/U6 complex was approximately that predicted from the efficiency of formation of its component U2/U6 and U4/U6 crosslinks (*13*). Assuming that single crosslinks form at ~1 percent efficiency (*10*), these values further suggest that the majority of U4/U6 complexes in HeLa nuclear extracts are in complexes

D. A. Wassarman is a graduate student and J. A. Steitz is a professor and investigator of the Howard Hughes Medical Institute in the Department of Molecular Biophysics and Biochemistry, Yale University School of Medicine, 295 Congress Avenue, New Haven, CT 06536.

with U2. The U2/U4/U6 crosslinked complex was also observed on RNA (Northern) blots of total crosslinked RNA (see below). Identification of a U2/U4/U6 crosslinked complex demonstrates that U6 can simultaneously associate with U2 and U4.

We have not mapped the positions of the crosslinks within the U2/U4/U6 complex, but since photoreversal generated complexes that comigrated with U4/U6 and U2/U6 complexes on two-dimensional gels, the doubly crosslinked complex seems likely to involve the base pairing interactions previously characterized for the singly crosslinked species (8, 9) (Fig. 1, longer exposure). This conclusion is supported by affinity selection with biotinylated complementary 2′-*O*-methyl oligoribonucleotides. An oligonucleotide complementary to the region of U2 (BU2b, nucleotides 30 to 43) (*14*) that is involved in base-pairing with the branch site selected both U2/U6 and U2/U4/U6 crosslinked complexes (*13*). Oligonucleotides complementary to regions of U4 (BU4a, nucleotides 1 to 20) (*15*) and U6 (BU6d, nucleotides 57 to 74) (*15*) that are involved in intermolecular U4-U6 stem II base pairing (*16*) did not select either U4/U6 or U2/U4/U6 crosslinked complexes, but BU6d did select the U2/U6 complex (Fig. 2B). Mapping of the U4/U6 crosslink in vitro (*8*) and in vivo (*13*) to the stem I helix (U4 nucleotides 56 to 63, U6 nucleotides 49 to 56) therefore suggests that melting of stem I is required for stem II dissociation and oligonucleotide hybridization.

The U1 and U2 complexes that remained in the well after the first dimension of electrophoresis (Fig. 1) may represent crosslinks to hnRNA in the extract. We also detected an abundant internally crosslinked U1 that has already been characterized (*17*).

Crosslinking of U1, U2, U5, and U6 snRNA's to pre-mRNA during in vitro splicing. To identify snRNA interactions with pre-mRNA, we added a biotinylated splicing substrate containing a portion of the adenovirus major late transcript (*18*) to HeLa nuclear extracts (Fig. 2A). Interactions that occur at different stages of splicing were captured by irradiating the reaction mixture with 365-nm light in the presence of psoralen, after an initial 30-minute incubation without psoralen or irradiation. Splicing efficiency is not significantly affected by the presence of psoralen (*13*). The snRNA/pre-mRNA crosslinked complexes were isolated by sequential selection, first with antibodies to m_3G (directed against spliceosomal snRNA's) and then with streptavidin (directed against biotiny-

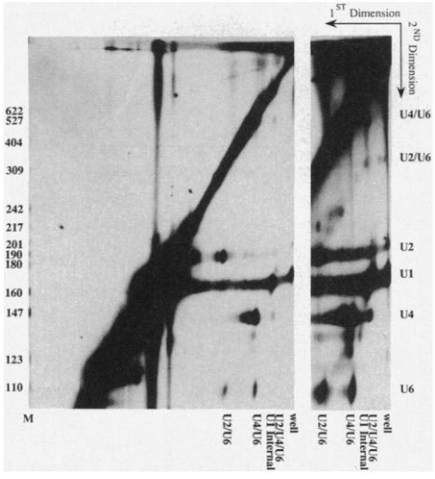

Fig. 1. Identification of endogenous snRNA-snRNA interactions in a HeLa nuclear extract. A reaction mixture containing 60 percent HeLa nuclear extract [prepared with 30 mM KCl in buffer D (*48*)], 0.5 mM ATP, 3.2 mM $MgCl_2$, and AMT (psoralen) at 20 μg/ml (HRI Associates) was irradiated at 365 nm for 10 minutes on ice (*9*). The snRNA's were immunoprecipitated with a monoclonal antibody to m_3G (Oncogene Sciences) (*49*), labeled at the 3′ end with T4 RNA ligase and [5′-^{32}P]pCp (*50*), and then fractionated on a 6 percent denaturing polyacrylamide gel in the first dimension. The gel lane was irradiated at 254 nm for 20 minutes at 4°C (*9*), and the resulting reversed RNA's were resolved on a 6 percent gel in the second dimension. The positions of the snRNA's and incompletely reversed complexes are indicated on the right, crosslinked RNA's are labeled at the bottom, and the sizes of DNA markers (M) (^{32}P-labeled Msp I digest of pBR322) in nucleotides are given on the left (New England Biolabs). Different exposures of the same gel are shown.

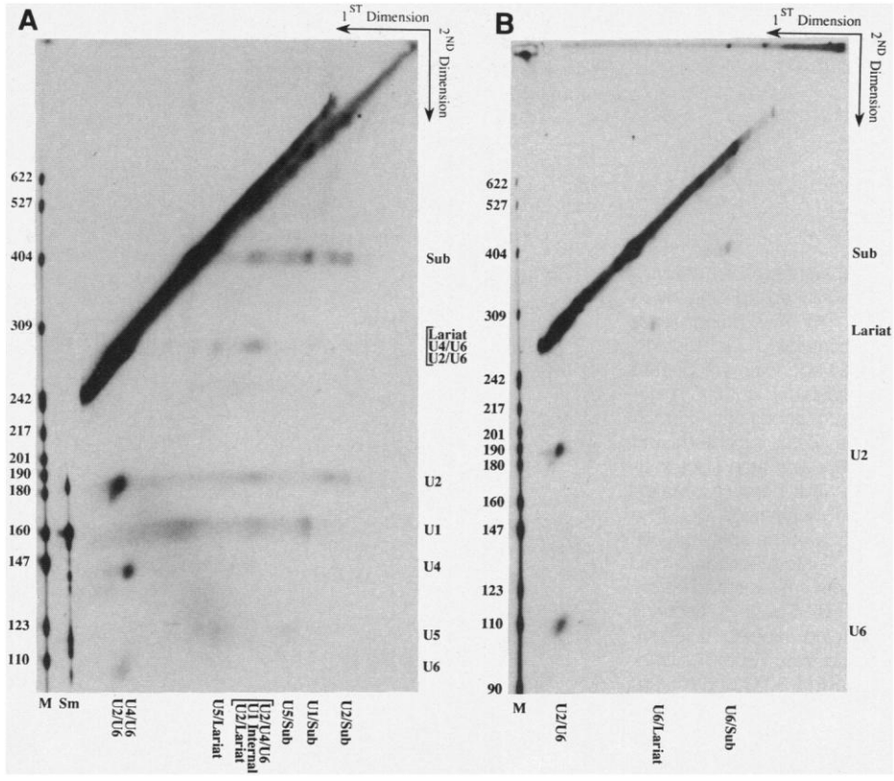

Fig. 2. Interactions of snRNA's with pre-mRNA during in vitro splicing. (**A**) A HeLa nuclear extract was incubated at 30°C with a biotinylated adenovirus major late splicing substrate (*18, 51*) under standard splicing conditions (60 percent extract, 0.5 mM ATP, 3.2 mM $MgCl_2$, and 20 mM creatine phosphate) for 30 minutes. Psoralen was then added to 20 μg/ml, and the mixture was exposed to 365-nm light while being incubated at 30°C for another 60 minutes; during this period, psoralen was added to 20 μg/ml every 15 minutes. Crosslinked complexes containing an snRNA and splicing substrate were sequentially selected, first by immunoprecipitation with antibodies to m_3G and then with streptavidin agarose (*15*). Selected RNA's were labeled at the 3′ end and fractionated on a two-dimensional gel as described (Fig. 1), except that 4 percent gels were used in both dimensions. RNA's were identified on the basis of their mobilities relative to the DNA markers (M) labeled on the left and the 3′ end-labeled α-Sm immunoprecipitated RNA (Sm) fractionated in the second dimension (*52*). The positions of snRNA's, splicing substrate (406 nts), excised lariat, and incompletely reversed complexes are labeled on the right; crosslinked complexes are labeled at the bottom. Sub, substrate. (**B**) A HeLa nuclear extract was incubated with the adenovirus substrate under standard splicing conditions for 30 minutes. Psoralen was added to 20 μg/ml, and the reaction was crosslinked for 10 minutes on ice. U6-containing complexes were affinity-selected with a biotinylated 2′-*O*-methyl oligoribonucleotide complementary to nucleotides 57 to 74 of U6 snRNA (BU6d) (*15*). Selected RNA's were analyzed as in (A).

lated pre-mRNA residues). Because U6 has a γ-methyl cap (*19*) and is only indirectly immunoprecipitable through association with U4, it was separately selected from total crosslinked RNA with the BU6d 2′-O-methyl oligonucleotide (Fig. 2B).

Two-dimensional gel fractionation (Fig. 2) of the selected RNA's revealed that U1, U2, U5, and U6 form crosslinks with the pre-mRNA and U2, U5, and U6 form crosslinks with the excised lariat intron. Low levels of endogenous U4/U6, U2/U6,

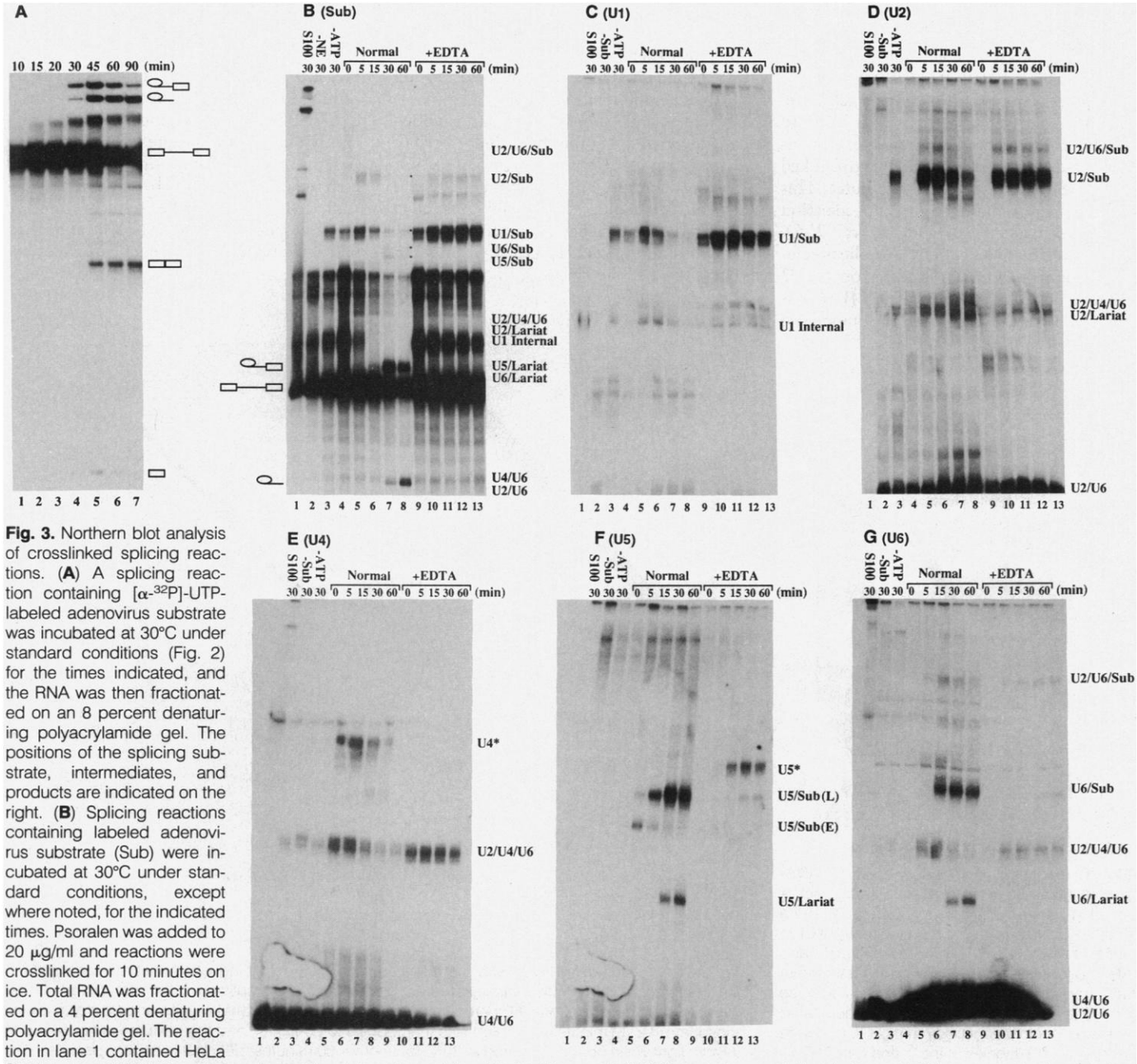

Fig. 3. Northern blot analysis of crosslinked splicing reactions. (**A**) A splicing reaction containing [α-^{32}P]-UTP-labeled adenovirus substrate was incubated at 30°C under standard conditions (Fig. 2) for the times indicated, and the RNA was then fractionated on an 8 percent denaturing polyacrylamide gel. The positions of the splicing substrate, intermediates, and products are indicated on the right. (**B**) Splicing reactions containing labeled adenovirus substrate (Sub) were incubated at 30°C under standard conditions, except where noted, for the indicated times. Psoralen was added to 20 μg/ml and reactions were crosslinked for 10 minutes on ice. Total RNA was fractionated on a 4 percent denaturing polyacrylamide gel. The reaction in lane 1 contained HeLa S100 extract (*48*) instead of nuclear extract; lane 2 contained buffer D (*48*) instead of nuclear extract; lane 3 had no added ATP or creatine phosphate; and lanes 9 to 13 contained 2.5 mM EDTA and no $MgCl_2$. Dots to the right of lane 8 denote complexes that were isolated for use in Figs. 4 and 5. The positions of crosslinked complexes, identified by comigration of substrate (B) and snRNA (C to G) hybridization signals, are indicated on the right and uncrosslinked substrate and lariats on the left. Sub, substrate. (**C** to **G**) Splicing, crosslinking, and electrophoresis were performed exactly as in (B) except with unlabeled adenovirus substrate; each lane 2 corresponds to a reaction mixture without substrate. The fractionated RNA's were transferred to nylon membrane and probed for spliceosomal snRNA's with in vitro–transcribed antisense RNA's (*53*) (Zeta-Probe GT, Bio-Rad Laboratories). The U2/U6 and U4/U6 complexes at the bottom of (G) are resolved on lighter exposures. In (E) and (F), uncharacterized crosslinks are denoted by a star, and, in (F), late and early U5 complexes are denoted by (L) and (E). The relative abundance of the different snRNA/pre-mRNA crosslinks is best estimated from (B) (labeled substrate), where there is a single uniform source of signal, and not by Northern blot analysis, where the snRNA probe lengths and the blot exposure times are different. For example, at 60 minutes the U1, U2, U5, and U6 crosslinks to the pre-mRNA are present in approximately equal amounts. The experiment shown was performed with a single extract, and corresponding lanes on the Northern blots are samples from the same reaction. Similar results were obtained in three different experiments. U1 probing was performed after removal of the U2 probe, and U4 probing was performed after removal of the U5 probe.

and U2/U4/U6 complexes (which represent background in the selection procedure) were also present. The U2/U4/U6, U2/lariat, and internal U1 crosslinks comigrate (Fig. 2A), but were identified on the basis of Northern blot analyses (Fig. 3). This method was also used to confirm the other snRNA/pre-mRNA crosslinks.

No crosslinks were observed to the 5′ exon, lariat intermediate, or spliced product. The absence of crosslinks is consistent with results from Lamond *et al.* (*14, 15*), who showed that 2′-*O*-methyl affinity selection of U2, U4, or U6 from splicing reactions co-selected pre-mRNA and excised intron but not splicing intermediates. Similarly, Sawa and Shimura (6) did not detect snRNA interactions with splicing intermediates by UV crosslinking. The lack of detectable psoralen crosslinks to the free 5′ exon and lariat intermediate may be due to the transient existence of these RNA species. Thus, intermediates detected on fractionation of splicing reactions may be molecules that are unable to proceed from the first to the second step of splicing. To attempt to capture snRNA crosslinks with splicing intermediates, we used heat-treated HeLa extracts, which are reported to accumulate free 5′ exon and lariat intermediate (*20*); however, these experiments were unsuccessful because the system was slightly leaky (producing a small amount of product) and the first step of splicing was too inefficient (*13*).

To determine the kinetics of interactions between snRNA's and pre-mRNA during splicing, we performed crosslinking at various times in the reaction (Fig. 3, B to G). Samples were irradiated on ice to stabilize the assembled complexes and to prevent further processing. After gel fractionation of total RNA, crosslinked ^{32}P-labeled adenovirus pre-mRNA substrate was visualized directly (Fig. 3B) and snRNA crosslinks with unlabeled substrate were monitored by Northern blot analyses (Fig. 3, C to G). Comigration of snRNA and pre-mRNA bands confirmed the interactions identified by two-dimensional gel electrophoresis and also revealed less abundant or transient interactions. As negative controls, crosslinking was analyzed in HeLa S100 extracts (Fig. 3, B to G, all lanes 1) and in reactions lacking extract (Fig. 3B, lane 2) or substrate (Fig. 3, C to G, all lanes 2). Fractionation of an uncrosslinked splicing reaction (Fig. 3A) showed that 5′ exon and lariat intermediate first appeared between 15 and 20 minutes of incubation (lanes 2 and 3), whereas excised lariat intron and spliced product appeared after 30 minutes (lane 4).

The U2/U6 and U4/U6 crosslinked complexes were prominent (Fig. 3, D, E, and G) because of their abundance in HeLa nuclear extracts. The doubly crosslinked U2/U4/U6 complex initially increased in abundance but then decreased during the splicing reaction. In the presence of EDTA, which allows spliceosome assembly but no cleavage (*21*), only the initial incubation-dependent increase occurred; this finding demonstrates that splicing is required to reduce the concentration of the U2-U4-U6 complex (Fig. 3, D, E, and G; compare lanes 4 to 8 with 9 to 13). We conclude that the preformed U2-U4-U6 complex is an active component of the splicing machinery in vitro.

No snRNA/pre-mRNA crosslinks were observed in the S100 extracts (Fig. 3, C to G, all lanes 1), which contain nearly the same concentration of splicing snRNP's as nuclear extracts but are inactive for splicing because they lack the protein factor ASF/SF2 (*22*). This control demonstrates that the crosslinks with snRNA's are not fortuitous, but splicing-dependent. However, the pre-mRNA did form multiple, presumably internal, crosslinks even in the absence of extract (Fig. 3B, lane 2). These crosslinks disappeared on incubation with extract under active splicing conditions, but not when splicing was inhibited by EDTA (Fig. 3B; compare lanes 4 to 8 with 9 to 13). U1 was the first snRNA to crosslink strongly to the pre-mRNA; crosslinking occurred even on ice (Fig. 3, B and C, lanes 4). Upon incubation at 30°C, U1 crosslinking peaked at 5 minutes and then decreased with time (Fig. 3, B and C, lanes 5 to 8). U2 did not crosslink to the pre-mRNA on ice, but on incubation at 30°C it had a crosslinking profile similar to that of U1 (Fig. 3, B and D, lanes 4 to 8). A U2/U6/pre-mRNA doubly crosslinked complex appeared at 5 minutes, reached a peak at 15 minutes, and then declined (Fig. 3, B, D, and G, lanes 4 to 8). One U5 crosslink to the pre-mRNA [U5(E)] was weak on ice, became more prominent after 5 minutes at 30°C, and gradually decreased over the course of splicing; a second, more abundant, U5 crosslink [U5(L)] appeared after 5 minutes and then became increasingly prominent over the course of the experiment (Fig. 3, B and F, lanes 4 to 8). Unlike the U1, U2, and U5 crosslinks to the pre-mRNA, which appear gradually, the U6/pre-mRNA crosslink was not detectable at 10 minutes (*13*) but appeared suddenly at 15 minutes and remained relatively constant thereafter (Fig. 3, B and G, lanes 4 to 8). After the second step of splicing, U2, U5, and U6 crosslinks to the excised lariat intron were detected (Fig. 3, D, F, and G, lanes 7 and 8). We did not detect U4 crosslinking to the pre-mRNA (Figs. 2A and 3E). However, U4 did form a crosslink with an unidentified partner; this interaction requires active splicing (not simply spliceosome assembly), because the crosslink was not observed when splicing was inhibited by EDTA [Fig. 3E; compare lanes 4 to 8 with 9 to 13 (U4*)].

In the absence of added ATP, U1 and U2 formed crosslinks with the pre-mRNA, whereas U5 and U6 did not (Fig. 3, B to D and F and G, lanes 3). The U2 crosslink was unexpected because stable association of U2 with the pre-mRNA has been shown to be ATP-dependent (*1*). In the presence of EDTA, the amount of crosslinking of U1, U2, and U2/U6 to the pre-mRNA did not decrease (Fig. 3, B to D and G, lanes 9 to 13). The faster migrating U5/pre-mRNA crosslinked complex [U5(E)] formed weakly and exhibited kinetics similar to that of the

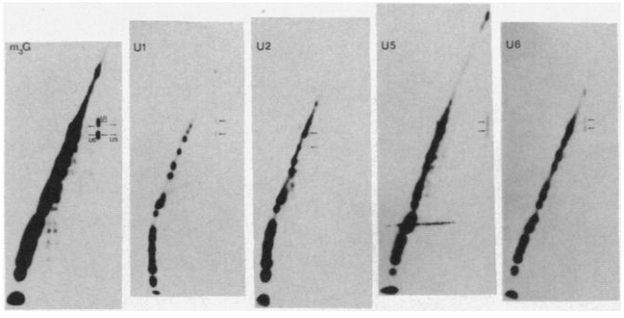

Fig. 4. Mapping of crosslinks to substrate RNase T1 fragments. A HeLa nuclear extract was incubated with [α-^{32}P]GTP-labeled adenovirus substrate for 40 minutes under standard splicing conditions (Fig. 2) and then crosslinked for 10 minutes on ice with 20 μg/ml of psoralen. U1/pre-mRNA and U2/pre-mRNA complexes were isolated by gel purification (complexes marked by dots in Fig. 3B) and U5 and U6 complexes were isolated from total crosslinked RNA by affinity selection with the biotinylated 2′-*O*-methyl oligonucleotides BU5Ae and BU6d, respectively (*14, 15*). (BU5Ae, which is complementary to nucleotides 69 to 87 of U5 RNA, has the sequence BBBBUIIIUUAAIACUCAIAIUU, where B denotes 2′-deoxycytidine residues that are sites of biotinylation, and I denotes 2′-*O*-methyl inosine.) In addition, all of the crosslinked complexes were co-selected by immunoprecipitation with antibodies to m_3G so that they could be directly compared (panel m_3G). Isolated complexes were digested to completion with RNase T1 (*8, 54*) and fractionated on a two-dimensional gel as described (Fig. 1) except that a 20 percent denaturing polyacrylamide gel was used in both dimensions. The U2 fragments are obscured by the diagonal in the m_3G panel. Arrows indicate the positions of photoreversed substrate RNase T1 fragments. In the m_3G panel, U6, U1, and U5 crosslinked fragments correspond to the left, middle, and right sets of horizontal arrows, respectively.

standard splicing reaction (Fig. 3F, lanes 9 to 13). The slower migrating U5/pre-mRNA complex [U5(L)] and the U6/pre-mRNA complex were almost undetectable in the presence of EDTA. Instead, a unique U5 complex appeared at late time points [Fig. 3F, lanes 11 to 13 (U5*)]. Perhaps the stable association of U1 and U2 with the pre-mRNA in the presence of EDTA blocked the site that normally interacts with U5, resulting in an aberrant U5 interaction.

Mapping of crosslinks to conserved regions in the snRNA's and pre-mRNA. Mapping of crosslinks on the adenovirus pre-mRNA substrate was performed with uniformly [α-^{32}P]GTP (guanosine triphosphate)-labeled substrate so that each RNase T1 fragment would be end-labeled. After incubation of splicing reactions for 40 minutes and subsequent addition of psoralen, crosslinked complexes of snRNA and pre-mRNA were isolated by immunoprecipitation with antibodies to m_3G, by affinity selection with 2′-O-methyl oligonucleotides to U5 (BU5Ae) or U6 (BU6d), or by gel purification of U1/pre-mRNA and U2/pre-mRNA complexes (marked by dots in Fig. 3B). Each selected complex was then digested with ribonuclease (RNase) T1 and fractionated on a two-dimensional gel (Fig. 4). Substrate fragments that contain crosslinks migrate aberrantly in the first dimension, and lie off the diagonal after photoreversal and fractionation in the second dimension. Because photoreversal is not complete, two labeled RNase T1 fragments appear: a slower species containing a psoralen monoadduct and a faster species devoid of psoralen, which migrates to the position expected for its size.

The U1, U5, and U6 RNA's all formed crosslinks with the same region of the pre-mRNA because their faster RNase T1 fragments comigrated in the second dimension (Fig. 4). Alkali hydrolysis of the oligonucleotide crosslinked to U1 identified it as a 16-nucleotide (nt) intron fragment that begins 6 nts downstream of the 5′ splice site (*13*). Similar analysis showed that U2 was crosslinked to a 14-nt RNase T1 fragment that covers the branch site (*13*). Monoadduct-containing oligonucleotides arising from the U1, U5, and U6 crosslinks did not comigrate in the second dimension, which suggests that they formed crosslinks at different positions within the 16-nt fragment. Alkali hydrolysis of the U1 monoadduct-containing fragment mapped the crosslink to U^9 of the intron (*13*). The U2, U5, and U6 crosslinks to the pre-mRNA and to the excised lariat intron could not be mapped to a single nucleotide because of the low yields of their respective oligonucleotides. However, it seems likely that U5 and U6 would make the same contacts with the lariat as those we have mapped for the pre-mRNA because (i) crosslinks to the excised lariat can only involve intron sequences, and (ii) previous UV crosslinking data (6) indicate that U6 binds intron sequences near the 5′ splice site throughout the reaction.

Inspection of the diagonal analyses (Fig. 4) also provides an estimate of the size of each unlabeled snRNA RNase T1 fragment

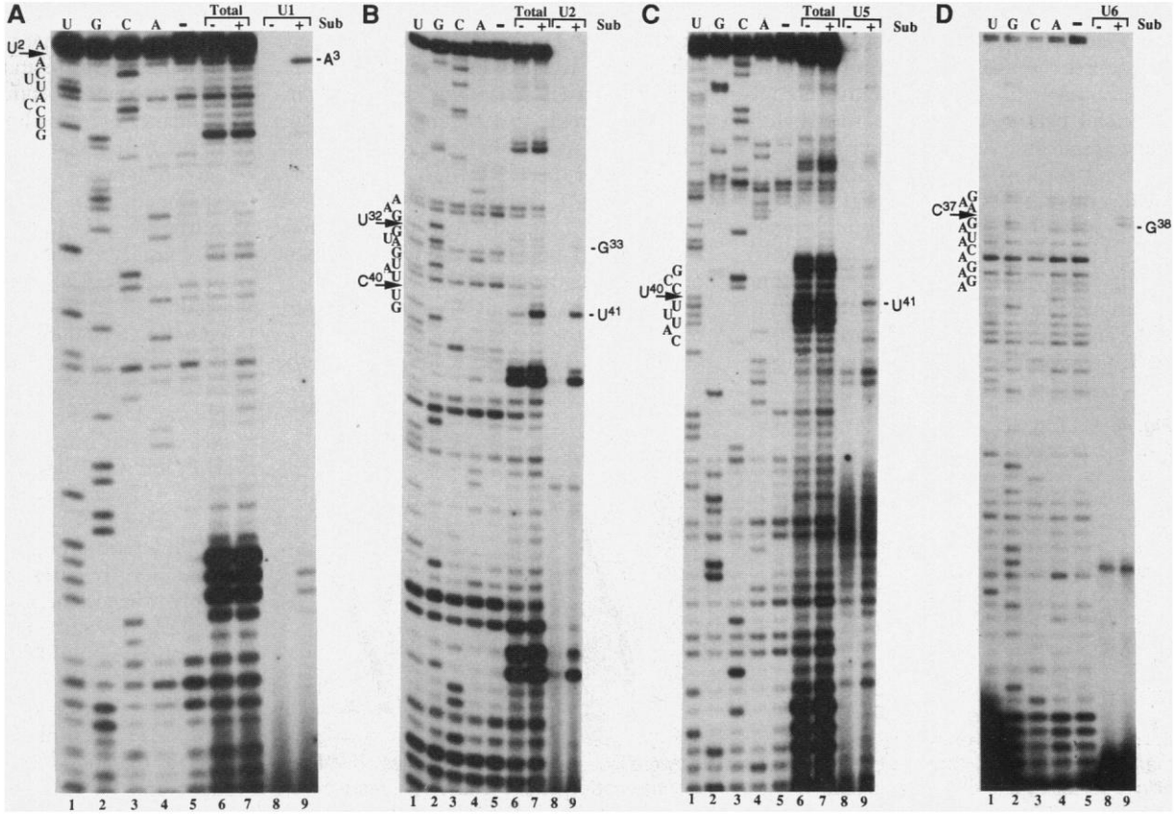

Fig. 5. Mapping of snRNA crosslinks by primer extension. A HeLa nuclear extract was incubated with or without a uniformly labeled adenovirus pre-mRNA substrate for 40 minutes under standard splicing conditions (Fig. 2) and then crosslinked for 10 minutes on ice with psoralen at 20 μg/ml. After fractionation on a 4 percent gel, snRNA/pre-mRNA complexes similar to those indicated by dots in Fig. 3B were excised along with the equivalent region of the gel containing extract crosslinked without substrate. Primer extension was performed on the crosslinked complexes with an appropriate ^{32}P-labeled oligonucleotide primer complementary to $U1^{64–75}$ (**A**), $U2^{79–98}$ (**B**), $U5^{84–104}$ (**C**), or $U6^{90–104}$ (**D**) (*55*). The reactions were then incubated with RNase A to digest the labeled substrate. Lanes 1 to 5 contain dideoxy sequencing reactions on nuclear extract RNA generated with the same primer. Lanes 6 and 7 show primer extensions with total RNA from reactions incubated without (−) or with (+) pre-mRNA, respectively [the reactions corresponding to lanes 6 and 7 of (D) are not shown in this particular gel, but were included on replicate gels]. Primer extension products from gel-purified bands derived from these same two reactions are shown in lanes 8 and 9. SnRNA sequences on the left correspond to those in Fig. 6A; arrows indicate the deduced positions of the psoralen crosslinks, which are based on the position of stops indicated on the right. Other stops in lane 9 were eliminated as potential crosslinking sites because they either occur at A residues or are incompatible with the sizes of the snRNA RNase T1 oligonucleotides deduced from Fig. 4.

that has become crosslinked. The U2 and U6 crosslinked fragments migrated close to the diagonal, an indication of small snRNA oligonucleotides, whereas the U1 and U5 crosslinks migrated farther from the diagonal, an indication of large and very large oligonucleotides, respectively. RNase T1 digestion yields three large products in the case of U1 (11, 12, and 13 nts), and one large product in the case of U5 (26 nts).

Primer extension mapping was used to locate the crosslink position within each snRNA (Fig. 5). Crosslinked snRNA/pre-mRNA complexes and comigrating control RNA from reactions incubated and crosslinked without pre-mRNA were isolated by gel purification (complexes marked by dots in Fig. 3B). Reverse transcripts from a 5′ end-labeled oligonucleotide primer complementary to the 3′ end of an snRNA terminate one nucleotide 3′ to the position of a psoralen crosslink. Bands that are enhanced in the experimental (+) versus the control (−) lanes locate the crosslink (compare lanes 8 and 9). Primer extension also detects numerous psoralen monoadducts when total RNA is analyzed (lanes 6 and 7). A subset of these monoadducts is enhanced by the presence of pre-mRNA; for example, nucleotides within the region of U2 that base pair with the branch site (Fig. 5B; compare lanes 6 and 7).

The U1 and U2 crosslinks with the pre-mRNA mapped to snRNA positions anticipated on the basis of previous studies (*1*). The U1 crosslink mapped to nucleotide U^{2} (within a 12-nt RNase T1 fragment) (Fig. 5A), which lies across from the crosslinked uridine residue in the pre-mRNA when the 5′ end of U1 is base-paired to the 5′ splice site (Fig. 6A). The U2 crosslink mapped to nucleotide U^{32} (within a 2-nt RNase T1 fragment) and nucleotide C^{40} (within a 6-nt RNase T1 fragment) (Fig. 5B), both of which have the potential to crosslink to the mapped pre-mRNA RNase T1 fragment when U2 is base paired to the branch site (Fig. 6A). Although only the U^{32} crosslink was predicted by diagonal analysis (Fig. 4), the diffuse nature of the U2/pre-mRNA crosslinked band on Northern blots suggests that U2 forms multiple crosslinks with the intron branch region (Fig. 3D).

The U5 crosslink mapped to nucleotide U^{40} (within a 26-nt RNase T1 fragment) (Fig. 5C) in the 9-nt invariant loop. This places U5 at the 5′ splice site where nucleotides 5 to 9 of the loop (nucleotides 41 to 45 of human U5) have the potential to base pair to consensus 5′ splice site intron nucleotides 1 to 5 (Fig. 6A). Newman and Norman have recently suggested that in *S. cerevisiae*, nucleotides 5 and 6 of the U5 invariant loop can pair with nucleotides −2 and −3 of 5′ exons (*4*). This orientation of U5 is not compatible with the major crosslink we observe; however, the weaker U5/pre-mRNA crosslink [Fig. 3F, U5(E)], whose kinetics parallels that of the U1/pre-mRNA crosslink, may reflect the predicted U5 interaction with 5′ exon sequences (*4*).

The U6 crosslink mapped to nucleotide C^{37} (within a 4-nt RNase T1 fragment) (Fig. 5D), adjacent to a region that is complementary to nucleotides 2, 5, 6, and 7 of the adenovirus intron (Fig. 6A). The potential base pairs involve nucleotides 1,

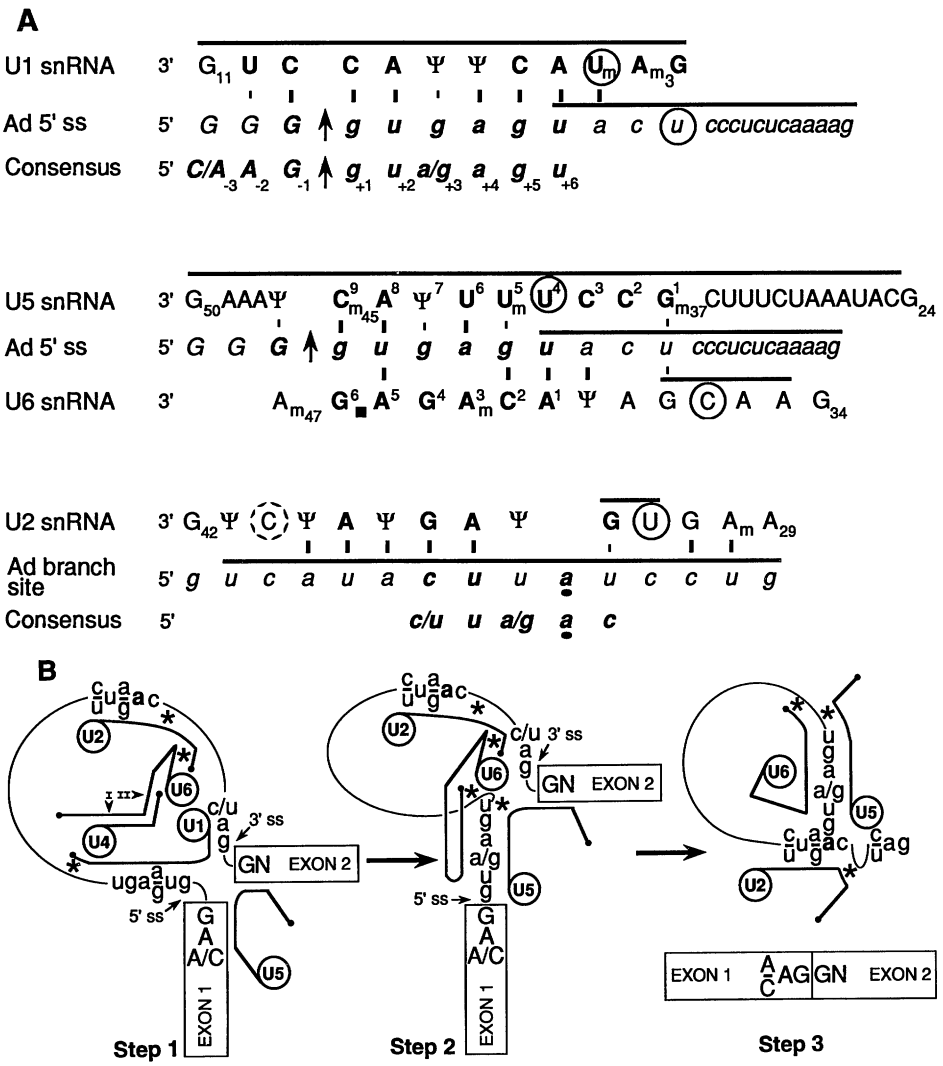

Fig. 6. A model for snRNA interactions with pre-mRNA during splicing. (**A**) The snRNA's and adenovirus pre-mRNA are shown in a configuration that places psoralen crosslinked nucleotides in close proximity. Pre-mRNA sequences are written in italics with the 5′ exon in uppercase and the intron in lowercase. Phylogenetically conserved sequences within the human snRNA's (*56*) and the adenovirus pre-mRNA are indicated in bold type. Consensus sequences for mammalian 5′ splice sites (*57*) and branch sites are also shown. Circled nucleotides denote specific sites of psoralen crosslinking determined by primer extension or sequencing of RNase T1 fragments, and solid lines indicate crosslinked RNase T1 fragments. Nucleotide positions within the human snRNA's and the 5′ splice site are labeled by subscripts. Superscripts are used to label nucleotides within the U5 invariant loop (*4*) and the U6 hexanucleotide sequence. Methylated residues are labeled by a subscript m, and Ψ denotes a pseudouridine. The 5′ splice site is marked by an arrow and the branch point adenosine by a dot. A black square indicates the position of an intron in U6 from the yeast *Rhodosporidium dacryoidum* (*39*). (**B**) SnRNA-pre-mRNA interactions at three steps during the splicing reaction, as determined by psoralen crosslinking. The snRNA's are drawn schematically with dots as 5′ caps and circles with the snRNA identity at the 3′ ends. Potential base pairing is indicated by parallel lines and asterisks indicate positions of crosslinking. Consensus pre-mRNA sequences are shown with exon in uppercase and intron in lowercase, with the branch point adenosine in bold type. Base pairing between the pre-mRNA and U1 and U5 in step 1 is drawn in an open configuration of a four-branch Holliday junction (*29*). Between steps 1 and 2, U5 shifts to contact 5′ intron sequences. Step 1 depicts snRNA crosslinking interactions at 5 minutes (Fig. 3, all lanes 5), step 2 at 15 minutes (all lanes 6), and step 3 at 30 minutes (all lanes 7). Stems within the U4 to U6 structure (*16*) are indicated in step 1.

2, and 5 of an invariant hexanucleotide sequence in U6 (ACAGAG). Our results are consistent with those of Sawa and Shimura, who reported UV crosslinking between the central domain of U6 (containing the ACAGAG) and a region encompassing the 5′ splice site of a pre-mRNA derived from the δ-crystallin gene (6). Mutagenesis of the yeast U6 hexanucleotide sequence causes severe splicing defects both in vitro and in vivo. In vitro, the most detrimental mutations are at the equivalent of human U6 positions C^{42} and A^{45}; the former blocks association of U6 with the spliceosome and the latter inhibits the second step of splicing, which causes accumulation of splicing intermediates (*23*). In vivo, all mutations at positions C^{42}, A^{43}, and A^{45} are lethal, whereas mutations at other hexanucleotide positions can be viable or temperature-sensitive (*24*). The yeast equivalent of U6 nucleotide A^{43}, in addition to C^{42} and A^{45}, has the potential to base pair with the 5′ splice site of yeast introns because position 4 is a highly conserved U, not an A as in mammals (*1*) (Fig. 6A). Base pairing between U1 and intron position 4 is not required in yeast (*25*), so base pairing with U6 may explain the conservation of this intron nucleotide.

A model for the sequential interactions of snRNA's with pre-mRNA during in vitro splicing. Splicing defects caused by mutations at consensus intron positions G^1, U^2, and G^5 are not completely suppressed by complementary mutations in the 5′ end of U1 (*25, 26*, and references therein). Thus, it has been argued that these nucleotides are recognized by additional splicing components that determine the location of 5′ splice site cleavage and allow efficient completion of the second step of the reaction. Our results suggest that these other factors are U5 and U6 snRNA's.

Our crosslinking data allow us to propose new base-pairing steps that may underlie the progression of snRNA interactions in the spliceosome. Additional base pairing steps may exist but not be revealed by our experiments because the adenovirus pre-mRNA may lack appropriate psoralen crosslinking sites. Conversely, the interactions may not be as extensive as those shown (Fig. 6A), they may involve base pairs other than the Watson-Crick type, or they may not occur at all for introns whose splice sites deviate from consensus sequences and therefore lack the ability to form the proposed interactions. Finally, we cannot rule out the possibility that some of the crosslinks observed involve dead-end products of in vitro splicing, but the kinetics of the crosslinks and their compatibility with observations cited below support our view that they are relevant to splicing.

Available data from both mammalian and yeast systems suggest a generalized in vitro splicing pathway in which sequentially:

1) The U1 RNA forms base pairs with consensus sequences at the 5′ splice site. We observed psoralen crosslinking of U1 on ice in the absence of U2, U4, and U6 crosslinking to pre-mRNA.

2) The U2 RNA forms base pairs with conserved branch site sequences. The unexpected crosslinking observed in the absence of ATP suggests that ATP is required not to form, but to stabilize, U2 snRNP binding. Association of U1 and U2 follows (*1*), thereby bringing together the 5′ and 3′ ends of the intron and allowing U1 to base pair with the absolutely conserved AG at the 3′ splice site (*2*). The U1 base pairing to the 5′ and 3′ splice sites may not be required because some pre-mRNA's can be spliced in vitro in the absence of the 5′ end of U1 RNA (*27*) or without the intron AG (*28*).

3) The pre-assembled U4-U5-U6 tri-snRNP joins to form the complete spliceosome, generating a Holliday-like structure (*29*) (Fig. 6B, step 1). U6 then contacts U2, probably through the base pairs previously characterized (*9*), and U5 interacts with exon sequences at the 5′ splice site. A U5/pre-mRNA crosslink with kinetics similar to that of U5(E) forms with substrates containing a photo-activatable crosslinking agent at position −2 of the 5′ exon (*30*); this observation supports the argument that the U5(E) crosslink reflects an interaction with 5′ exon sequences (Fig. 6B, step 1). Both the U5(E) and U2/U6 crosslinks with the pre-mRNA occur within 5 minutes of incubation, even in the presence of EDTA; it is conceivable that in vivo U2-U4-U5-U6 joins as a preformed complex, because crosslinking shows that U6 can simultaneously base pair with U2 and U4. Support for base pairing between the 3′ end of U6 and the 5′ end U2 (*5*) at this stage of mammalian spliceosome assembly comes from previous experiments showing that spliceosome assembly is: (i) drastically reduced when the 3′ end of U6 is mutated to disrupt base pairing with U2 (*31*); and (ii) stalled after association of U1 and U2 when the 5′ end of U2 is blocked by oligonucleotide hybridization (*32*). However, in *Saccharomyces cerevisiae* this particular U2/U6 interaction is tolerant to mutation (*5, 33*), and U5 may not be absolutely required for the first step of splicing (*34*). Furthermore, Madhani and Guthrie have proposed a new type of U2/U6 pairing that is essential for cell growth and efficient splicing in yeast (*35*).

4) The base pairing between U1 and the 5′ splice site is unwound, which allows U5 to shift and base pair with intron sequences at the 5′ splice site (Fig. 6B, step 2). The kinetics of the two psoralen crosslinks to U5 indicates that they are mutually exclusive and that the earlier (E) is a precursor to the later (L). This putative later interaction of U5 with 5′ intron sequences explains the conservation of nucleotides 7 to 9 in the invariant loop, whereas the work of Newman and Norman accounts for the conservation of nucleotides 3 to 6 (*3, 4*). U1 may completely dissociate from the spliceosome at this stage. Compensatory mutations in yeast U1 that suppress mutations of the conserved AG at the 3′ splice site restore only the first step of splicing (*2*), which suggests that some other factor recognizes this dinucleotide in the second step.

5) The intermolecular U4-U6 base pairing is unwound, which releases U4 from U6. The U4 RNA is not required for subsequent steps (*36*). Its dissociation may allow the previously masked U6 to play a catalytic role, as proposed (*37*) on the basis of its high sequence conservation and on the presence of mRNA-like introns in functionally important regions of U6 in several species of yeast (see Fig. 6A) (*38, 39*).

6) The U6 RNA forms base pairs with conserved intron sequences at the 5′ splice site. This interaction is not mutually exclusive with U5-intron base pairing (Fig. 6A), but there is no evidence for simultaneous pairing. The U6/pre-mRNA crosslink is the last to occur before the appearance of splicing intermediates, which suggests that this U6 interaction triggers the first step of splicing (see below). Accordingly, a study of yeast pre-mRNA sequences showed that chemical modification of intron position U^2 at the 5′ splice site had its greatest inhibitory effect on spliceosome assembly after release of U4 from U6 (*40*) (see Fig. 6A).

7) After inspection of the 5′ splice site by U1, U5, and U6, a catalytically active conformation is created, cleavage occurs at the 5′ splice site, and the second step of splicing proceeds rapidly. Spliced mRNA is then released from the spliceosome, with U2, U5, and U6 remaining base paired to the excised lariat intron (Fig. 6B, step 3).

U6 analogies with domain 5 of group II self-splicing introns. Nuclear pre-mRNA splicing and group II autocatalytic splicing proceed by an identical two-step transesterification mechanism that generates a lariat intermediate (*41, 42*). Thus, an evolutionary relation has been proposed in which spliceosomal snRNA's represent trans-acting fragments of an original self-splicing intron (*43*). Indeed, sequences at the splice sites exhibit conservation between the two systems, and several interactions between snRNA's and pre-mRNA in the spliceosome have similarities to intramolecular group II base pairing interactions. In particular, complementarity of U2 to the intron branch site mimics the structure of domain 6 of group II introns, in which the branch point adenosine residue bulges from

a helical stem (*41*). In addition, the functioning of the invariant loop of U5 has been suggested to be similar to that of the D3 loop of group II introns (*4*). The D3 loop contributes to 5′ splice site recognition by base pairing with exon sequences (the EBS1-IBS1 interaction) and can also base pair an adjacent nucleotide with the first nucleotide of the 3′ exon, an interaction required for 3′ splice site cleavage (*42*).

We propose that a functional analogy exists between spliceosomal U6 and domain 5 of group II introns. Jarrell *et al.* (*44*) have shown that when domain 5 is provided in trans to a half-molecule containing the 5′ exon and domains 1 to 3 of a group II intron, it allowed hydrolysis at the 5′ splice site. In addition, Koch *et al.* (*45*) have shown that only domain 1 is required for 5′ splice site hydrolysis by domain 5, which suggests that domain 1 contains the binding site for domain 5. These studies showed that domain 5 is necessary to activate the 5′ splice site and that, in the complete group II intron, the proximity of domains 5 and 6 may bring the branch point adenosine close to the 5′ splice site, thereby ensuring that the adenosine (rather than water) attacks in the first step of splicing. In those group II introns that are dispersed over several genomic sites and act in trans, domains 5 and 6 always reside on the same transcript (*46*). Finally, a group II intron has been identified within domain 5 of another group II intron (*47*).

The U6 RNA and domain 5 of group II introns share many properties: (i) Both are the most conserved elements of their respective systems (*16*, *41*); (ii) the region of U6 (nucleotides 40 to 56) that crosslinks to the 5′ splice site exhibits both sequence and potential structural similarity to domain 5 (the top half) of group II introns in subgroup A (*41*) (note that this region of U6 is partially masked in the presence of U4); (iii) the U6/pre-mRNA crosslink occurs just prior to 5′ splice site cleavage, which suggests that U6 triggers the first step of splicing as domain 5 does in group II introns; (iv) through its base pairing with U2 prior to 5′ splice site cleavage, U6 may bring the branch point adenosine close to the 5′ splice site, just as the linkage between domains 5 and 6 does in group II introns (see Fig. 6B, step 2); and (v) like domain 5, U6 in several species of yeast contains introns that are located within functionally important regions of the molecule (*38*, *39*). Characterization of additional crosslinking interactions in the spliceosome should reveal further parallels between snRNA's and functional domains of group II self-splicing introns.

REFERENCES AND NOTES

1. M. R. Green, *Annu. Rev. Cell Biol.* **7**, 559 (1991); C. Guthrie, *Science* **253**, 252 (1991); T. Maniatis and R. Reed, *Nature* **325**, 673 (1987); M. Rosbash and B. Seraphin, *Trends Biochem Sci.* **16**, 187 (1991); S. W. Ruby and J. Abelson, *Trends Genet.* **7**, 79 (1991); J. A. Steitz *et al.*, in *Structure and Function of Major and Minor Small Nuclear Ribonucleoprotein Particles*, M. L. Birnstiel, Ed. (Springer-Verlag, Berlin, 1988), pp. 115–154.
2. C. I. Reich, R. W. VanHoy, G. L. Porter, J. A. Wise, *Cell* **69**, 1159 (1992).
3. A. J. Newman and C. Norman, *ibid.* **65**, 115 (1991).
4. _____, *ibid.* **68**, 1 (1992).
5. B. Datta and A. M. Weiner, *Nature* **352**, 821 (1991); J. Wu and J. L. Manley, *ibid.*, p. 818.
6. H. Sawa and Y. Shimura, *Genes Dev.* **6**, 244 (1992).
7. J. P. Calvet and T. Pederson, *Cell* **26**, 363 (1981); J. P. Calvet, L. M. Meyer, T. Pederson, *Science* **217**, 456 (1982).
8. J. Rinke, B. Appel, M. Digweed, R. Lührmann, *J. Mol. Biol.* **185**, 721 (1985).
9. T.-P. Hausner, L. M. Giglio, A. M. Weiner, *Genes Dev.* **4**, 2146 (1990).
10. G. D. Cimino, H. B. Gamper, S. T. Isaacs, J. E. Hearst, *Annu. Rev. Biochem.* **54**, 1151 (1985).
11. K. Nakashima, E. Darzynkiewicz, A. J. Shatkin, *Nature* **286**, 226 (1980).
12. Labeling with [5′-^{32}P]pCp can misrepresent the abundance of the snRNA's because different 3′ end residues have different efficiencies as acceptors for pCp. In particular, U6 is underrepresented because a cyclic phosphate at the 3′ end of most U6 molecules prevents pCp labeling [E. Lund and J. E. Dahlberg, *Science* **255**, 327 (1992)].
13. D. A. Wassarman and J. A. Steitz, unpublished data.
14. S. M. L. Barabino, B. S. Sproat, U. Ryder, B. J. Blencowe, A. I. Lamond, *EMBO J.* **8**, 4171 (1989). All of the 2′-*O*-methyl oligonucleotides used in this study specifically select the targeted snRNA from total nuclear extract RNA (not shown). The BU5Ae 2′-*O*-methyl oligonucleotide was synthesized by J. Flory on an Applied Biosystems DNA synthesizer with phosphoramidite monomers purchased from EMBL [B. S. Sproat, A. I. Lamond, B. Beijer, P. Neuner, U. Ryder, *Nucleic Acids Res.* **17**, 3373 (1989)].
15. B. J. Blencowe, B. S. Sproat, U. Ryder, S. Barabino, A. I. Lamond, *Cell* **59**, 531 (1989).
16. D. A. Brow and C. Guthrie, *Nature* **334**, 212 (1988).
17. J. P. Calvet and J. A. Myers, *J. Mol. Biol.* **197**, 543 (1987).
18. D. Solnick, *Cell* **42**, 157 (1985).
19. R. Singh and R. Reddy, *Proc. Natl. Acad. Sci. U.S.A.* **86**, 8280 (1989).
20. A. R. Krainer and T. Maniatis, *Cell* **42**, 725 (1985).
21. S. M. Abmayr, R. Reed, T. Maniatis, *Proc. Natl. Acad. Sci. U.S.A.* **85**, 7216 (1988).
22. H. Ge and J. L. Manley, *Cell* **62**, 25 (1990); A. R. Krainer, G. C. Conway, D. Kozak, *ibid.*, p. 35.
23. P. Fabrizio and J. Abelson, *Science* **250**, 404 (1990).
24. H. D. Madhani, R. Bordonne, C. Guthrie, *Genes Dev.* **4**, 2264 (1990).
25. P. G. Siliciano and C. Guthrie, *ibid.* **2**, 1258 (1988).
26. B. Seraphin and M. Rosbash, *Cell* **63**, 619 (1990).
27. J. P. Bruzik and J. A. Steitz, *ibid.* **62**, 889 (1990).
28. B. C. Rymond and M. Rosbash, *Nature* **317**, 735 (1985); C. W. J. Smith, E. B. Porro, J. G. Patton, B. Nadal-Ginard, *ibid.* **342**, 243 (1989).
29. J. A. Steitz, *Science* **257**, 888 (1992).
30. J. Wyatt, E. J. Sontheimer, J. A. Steitz, in preparation.
31. T. Wolff and A. Bindereif, *EMBO J.* **11**, 345 (1992).
32. A. I. Lamond, B. S. Sproat, U. Ryder, J. Hamm, *Cell* **58**, 383 (1989).
33. O. E. Shuster and C. Guthrie, *Nature* **345**, 270 (1990).
34. B. Patterson and C. Guthrie, *Cell* **49**, 613 (1987).
35. H. D. Madhani and C. Guthrie, personal communication.
36. S-L. Yean and R-J. Lin, *Mol. Cell. Biol.* **11**, 5571 (1991).
37. C. Guthrie, *Am. Zool.* **29**, 559 (1989).
38. T. Tani and Y. Ohshima, *Nature* **337**, 87 (1989); C. Reich and J. A. Wise, *Mol. Cell. Biol.* **10**, 5548 (1990).
39. T. Tani and Y. Ohshima, *Genes Dev.* **5**, 1022 (1991).
40. B. Rymond and M. Rosbash, *ibid.* **2**, 428 (1988).
41. F. Michel, K. Umesono, H. Ozeki, *Gene* **82**, 5 (1989).
42. A. Jacquier, *Trends Bioch. Sci.* **15**, 351 (1990); _____ and N. Jacquesson-Breuleux, *J. Mol. Biol.* **219**, 415 (1991).
43. T. Cech, *Cell* **44**, 207 (1986); P. A. Sharp, *ibid.* **42**, 397 (1985); *Science* **254**, 663 (1991).
44. K. A. Jarrell, R. C. Dietrich, P. S. Perlman, *Mol. Cell. Biol.* **8**, 2361 (1988).
45. J. L. Koch, S. C. Boulanger, S. D. Dib-Hajj, S. K. Hebbar, P. S. Perlman, *ibid.* **12**, 1950 (1992).
46. Y. Chapdelaine and L. Bonen, *Cell* **65**, 465 (1991); M. Goldschmidt-Clermont *et al.*, *ibid.*, p. 135; V. Knoop, W. Schuster, B. Wissinger, A. Brennicke, *EMBO J.* **10**, 3483 (1991); B. Wissinger, W. Schuster, A. Brennicke, *Cell* **65**, 473 (1991).
47. D. W. Copertino and R. B. Hallick, *EMBO J.* **10**, 433 (1991).
48. J. D. Dignam, R. M. Lebovitz, R. G. Roeder, *Nucleic Acids Res.* **11**, 1475 (1983).
49. J. A. Steitz, *Methods Enzymol.* **180**, 468 (1989).
50. T. E. England, A. G. Bruce, O. C. Uhlenbeck, *ibid.* **65**, 65 (1980).
51. P. J. Grabowski and P. A. Sharp, *Science* **233**, 1294 (1986).
52. E. A. Lerner, M. R. Lerner, C. A. Janeway, J. A. Steitz, *Proc. Natl. Acad. Sci. U.S.A.* **78**, 2737 (1981).
53. D. L. Black and A. L. Pinto, *Mol. Cell. Biol.* **9**, 3350 (1989).
54. E. Garrett-Wheeler, R. E. Lockard, A. Kumar, *Nucleic Acids Res.* **12**, 3405 (1984).
55. A. J. Zaug, J. R. Kent, T. R. Cech, *Science* **224**, 574 (1984).
56. S. Gupta and R. Reddy, *Nucleic Acids Res.* **19**, 2073 (1991).
57. S. M. Mount, *ibid.* **10**, 459 (1982); Y. Oshima and Y. Gotoh, *J. Mol. Biol.* **195**, 297 (1987).

58. We thank K. Wassarman, K. Tyc, S. Seiwert, D. Toczyski, and other members of the Steitz laboratory for advice and criticism; J. Gall for the tutorial on drawing Holliday structures; and K. Wassarman, E. Sontheimer, and K. Tyc for critical reading of the manuscript. Supported by grant GM26154 from the National Institutes of Health.

27 May 1992; accepted 12 August 1992